Front. Chem. Sci. Eng. 2022, 16(5): 755–763
https://doi.org/10.1007/s11705-022-2137-3

RESEARCH ARTICLE

Lithium-based draw solute for forward osmosis to treat wastewater discharged from lithium-ion battery manufacturing

Rongzhen Chen, Xinfei Dong, Qingchun Ge (✉)

College of Environment and Safety Engineering, Fuzhou University, Fuzhou 350116, China

© Higher Education Press 2022

Abstract As draw solute is the core element of forward osmosis (FO) technology, here Li-Bet-Tf_2N synthesized from a customized ionic liquid betainium bis(trifluoromethylsulfonyl)imide ([Hbet][Tf_2N]) and Li_2CO_3 recovered from lithium-ion battery (LIB) wastes is proposed as a novel draw solute to treat Li^+-containing wastewater from LIB manufacturing through FO filtration. Having high dissociation ability and an extended structure, Li-Bet-Tf_2N generates a sufficiently high osmotic pressure to drive the FO filtration efficiently along with insignificant reverse solute diffusion. Li-Bet-Tf_2N produces a water flux of 21.3 $L\cdot(m^2\cdot h)^{-1}$ at 1.0 $mol\cdot L^{-1}$ against deionized water, surpassing conventional NaCl and $MgCl_2$ draw solutes with a higher water recovery efficiency and a smaller solute loss. Li-Bet-Tf_2N induces a more stable and higher water permeation flux with a 10.0% water flux decline than NaCl and $MgCl_2$ for which the water fluxes decline 16.7% and 16.4%, respectively, during the treatment of 2000 $mg\cdot L^{-1}$ Li^+-containing wastewater for 12 h. More remarkably, unlike other draw solutes which require intensive energy input and complicated processes in recycling, Li-Bet-Tf_2N is easily separated from water via solvent extraction. Reproducible results are achieved with the recycled Li-Bet-Tf_2N. Li-Bet-Tf_2N thus demonstrates a novel class of draw solute with great potentials to treat wastewater economically.

Keywords forward osmosis, lithium-ion battery, draw solution, lithium-containing wastewater, water treatment

1 Introduction

Currently rechargeable lithium-ion batteries (LIBs) are widely used in various fields such as electronic devices and electric vehicles [1–5]. Li-containing wastewater discharged from LIBs industry has become a severe environmental issue [6–8]. Traditional technologies face difficulties of incomplete contaminant removal, production of sludge wastes, heavy chemicals requirement and secondary pollution risks [9–11]. Forward osmosis (FO) has been widely used to treat metal ions-containing wastewater due to its complete removal for a wide range of contaminants, zero-pressure operation and low fouling tendency [12–14]. FO is therefore promising to treat Li-containing wastewater more efficiently than those conventional techniques [15–17]. However, the lack of a suitable draw solute from which the driving force is regenerated impedes the wide applications of FO technology.

Commercial substances, such as NaCl, $MgCl_2$, NH_4HCO_3 [18,19] have been proposed for FO draw solutes. However, the commercial draw solutes usually have severe salt leakage and are highly energy-consuming in recycling. Ge and Chung proposed that polyelectrolytes [20] and metal complexes [12] have high water flux and negligible salt flux as draw solution, while high-energy recycling is still a problem. Intelligent materials including nanoparticles [21], hydrogels [22] and ionic liquids [23] have been proposed to solve high-energy recycling, while the synthetic category generally faces challenges of low water permeation flux and low stability problem in the posttreatment.

In this study, we aim to design a novel class of Li-based draw solute from the wastes discharged from LIBs industry and use it to treat Li^+-containing wastewater through FO separation. From Li_2CO_3, a substance recovered from $LiCoO_2$ wastes discharged from LIBs industry [24,25], Li-Bet-Tf_2N has been synthesized via a simple neutralization reaction with [Hbet][Tf_2N] ionic liquid. The physicochemical properties and FO performance of Li-Bet-Tf_2N as a draw solute are systematically investigated [26]. The

Received May 31, 2021; accepted October 26, 2021

E-mail: qcge2015@fzu.edu.cn

application of Li-Bet-Tf_2N facilitated FO separation in Li-containing wastewater reclamation is extensively studied. The recycling of Li-Bet-Tf_2N via a simple solvent extraction strategy is evaluated. With higher water recovery efficiency and lower reverse solute diffusion in FO along with a simpler recycling process when compared with those reported draw solutes [22,23,27], Li-Bet-Tf_2N demonstrates its suitability and superiority as a novel class of draw solute, and thus promising to be used for other categories of wastewater treatment.

2 Experimental

2.1 Chemicals

Betaine hydrochloride ($[N^+(CH_3)_3CH_2COO^-]\cdot HCl$) (99%, Adamas), lithium sulfate monohydrate ($Li_2SO_4\cdot H_2O$) (99%, Adamas) and lithium carbonate (Li_2CO_3) (99%, Adamas) were purchased from Shanghai Titan Technology Co., Ltd. NaCl (99.5%, Adamas), $MgCl_2\cdot 6H_2O$ (98%, Adamas) were provided by Tianjin Fuchen Chemical Reagent Co., Ltd. Lithium bis(trifluoromethanesulfonyl)imide ($Li[(CF_3SO_2)_2N]$) (99%) was provided by Chengdu Ainahua Chemical Co., Ltd. All chemicals were used as received without further purification. Deionized water was produced by a Millipore ultrapure water system.

2.2 Li-Bet-Tf_2N synthesis

Betaine hydrochloride (25.0 mmol, 3.84 g) dissolved in 5 mL water was mixed with $Li[(CF_3SO_2)_2N]$ (25.0 mmol, 7.18 g) in 20.0 mL water. The mixture was stirred for 1 h at room temperature. [Hbet][Tf_2N] ionic liquid was synthesized instantly and the formed organic phase was below the aqueous phase. The [Hbet][Tf_2N] ionic liquid was then separated and washed with cold water. After that, Li_2CO_3 (12.5 mmol, 0.93 g) was added, and the mixture was continuously stirred for 30 min, followed by filtration to remove the excessive Li_2CO_3. Colorless crystalline Li-Bet-Tf_2N was obtained after vacuum dry with a yield > 99%.

2.3 Li-Bet-Tf_2N characterizations

Fourier transform infrared (FTIR) spectroscopy and proton nuclear magnetic resonance (NMR) were used to identify the chemical composition and functional groups of Li-Bet-Tf_2N, respectively. The FTIR iS10 Nicolet spectrometer equipped with Smart Omni-Transmission accessory was used for FTIR analysis, while a Bruker ACF300 (300 MHz) was used for NMR measurements. A SYP1003-III pertroleum product kinematic viscometer and a densitometer (DMA35, Anton Paar) were employed to measure the elution time and density of deionized water and Li-Bet-Tf_2N at 25 °C, respectively. The relative viscosity (η_r) of Li-Bet-Tf_2N to deionized water was obtained according to Eq. (1) [28]:

$$\eta_r = \frac{\eta}{\eta_0} = \frac{t\rho}{t_0\rho_0}, \tag{1}$$

where t and t_0 are the respective elution times of Li-Bet-Tf_2N and deionized water, while ρ and ρ_0 ($g\cdot cm^{-3}$) are the respective densities of Li-Bet-Tf_2N and deionized water.

A dynamic light scattering nanoparticle size analyzer (Brookhaven Instruments, NanoBrook Omni) was used to measure the hydrated radius of Li-Bet-Tf_2N in its aqueous solution. A conductivity meter (DDSJ-308F), pH meter (Horiba pH meter D-54, Japan) and a portable permeameter (Gonotec 3000, Germany) were deployed to evaluate the conductivity, acid-base property and osmotic pressure of Li-Bet-Tf_2N solution, respectively.

2.4 FO performance

FO tests were conducted on a lab-scale membrane system tailor-made by Suzhou Faith and Hope Membrane Technology Co., Ltd. A self-made flat sheet polyamide (PA) membrane was used in the FO system. Deionized water and Li_2SO_4 (0–2000 $mg\cdot L^{-1}$) solutions served as feed solutions, while Li-Bet-Tf_2N, NaCl and $MgCl_2$ were used as draw solutions. The initial volumes of the draw and feed solutions were fixed at 50 mL. The effective membrane area was 4.5 cm^2 and both the feed and draw solutions were pumped with an average flow velocity of 1.3 $cm\cdot s^{-1}$. A digital balance (BSA224S, Sartorius) was used to record the weight change of the draw solution during the tests. The reverse salt flux was converted from conductivities which were determined by a conductivity meter. All experiments were carried out at room temperature.

Water flux (J_w, $L\cdot(m^2\cdot h)^{-1}$)) was determined by the ratio of the weight changes of Li-Bet-Tf_2N solution over the product of membrane surface area and testing duration according to Eq. (2) [29]:

$$J_w = \frac{\Delta V}{A\Delta t}, \tag{2}$$

where ΔV (L) refers to the volume of permeation water collected in a predetermined time Δt (h) during the test, and A is the effective membrane surface area (m^2). The reverse solute flux, (J_s, $g\cdot(m^2\cdot h)^{-1}$) was calculated by Eq. (3) [29]:

$$J_s = \frac{C_t V_t - C_0 V_0}{A\Delta t}, \tag{3}$$

where C_t ($g\cdot L^{-1}$) and V_t (L) are the respective salt concentration and final volume of the feed solution after a certain period of time Δt (h), and C_0 ($g\cdot L^{-1}$) and V_0 (L) are the respective initial salt concentration and volume.

Li_2SO_4 feed solution at 2000 $mg\cdot L^{-1}$ was prepared by dissolving certain amount of Li_2SO_4 in deionized water.

Less concentrated feed solution was obtained by diluting the stock solution to a required concentration prior to use. The reverse diffusion of feed solute to the draw solution side was analyzed by inductively coupled plasma-optical emission spectroscopy (ICP-OES, Optima 7300DV, Perkin Elmer, USA).

3 Results and discussion

3.1 Synthesis and characterization of Li-Bet-Tf_2N

As shown in Fig. 1, Li-Bet-Tf_2N is synthesized through a one-pot reaction of [Hbet][Tf_2N] and Li_2CO_3 which is recovered from $LiCoO_2$ wastes (Fig. 1(a)). Unlike other recently proposed draw solutes, such as polyelectrolytes [20], hexavalent phosphazene salts [30], hydrogels [31], nanoparticles [22] which are usually synthesized from expensive raw materials, toxic solvents, or through complicated synthesis routes, Li-Bet-Tf_2N is synthesized more conveniently, economical and environmental friendly from a recycled material with a shorter synthetic route excluding toxic organic solvents.

FTIR spectra show a characteristic peak of O–H at 3415 cm^{-1} in both betaine monomer and Li-Bet-Tf_2N (Fig. 1(b)) [32]. The characteristic absorption of C=O stretching vibration appears at 1720 cm^{-1} in betaine, while it shifts towards low field to 1634 cm^{-1} in Li-Bet-Tf_2N due to the electron withdrawing effects of the cationic Li^+. The absorption peaks at 1334 and 1134 cm^{-1} which are only observed in Li-Bet-Tf_2N are from the symmetric and asymmetric stretching vibrations of S=O. The signal at 410 cm^{-1} in Li-Bet-Tf_2N is produced by the vibration of Li–O bond [33].

The protons in N–CH_2 (δ = 3.95 ppm) of Li-Bet-Tf_2N shift upfield relative to those in betaine (δ = 4.19 ppm) (Fig. 1(c)), due to reduced electron-withdrawing ability of the adjacent carboxyl group after combined with Li^+ ions. The resonances of protons in N–CH_3 are affected insignificantly from betaine (δ = 3.31 ppm) to the Li-Bet-Tf_2N product (δ = 3.32 ppm) because Li^+ has negligible effects on the terminal methyl groups. All these observations indicate that Li-Bet-Tf_2N is successfully synthesized.

3.2 Li-Bet-Tf_2N properties

Li-Bet-Tf_2N is soluble well in water and has a pH value of 7.5–8.6 at the concentration changing from 0.2 to 1.0 $mol \cdot L^{-1}$, suggesting good compatibility with the PA membrane and potential suitability to be an FO draw solute.

Figure 2 shows that Li-Bet-Tf_2N produces an osmotic pressure ranging from 13.0 to 64.8 bar when varying the concentration from 0.2 to 1.0 $mol \cdot L^{-1}$ (Fig. 2(a)). The osmotic pressure of Li-Bet-Tf_2N is clearly higher than that

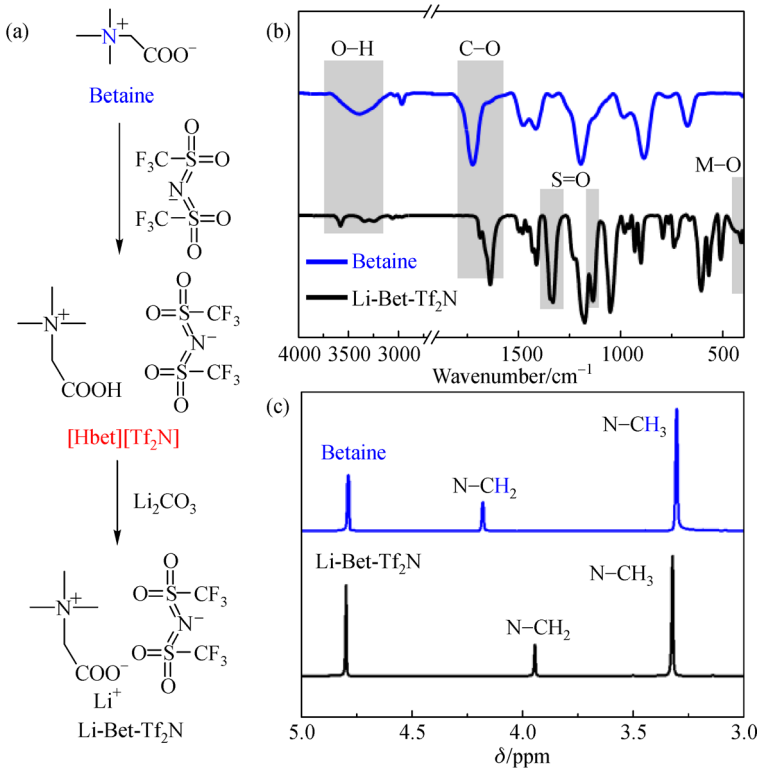

Fig. 1 (a) Synthesis scheme of Li-Bet-Tf_2N; (b) FTIR spectra of betaine and Li-Bet-Tf_2N; (c) ^1H NMR spectra of betaine and Li-Bet-Tf_2N.

of NaCl, but is slightly less than that of $MgCl_2$ at the same concentration. Li-Bet-Tf_2N, same as $MgCl_2$, is able to ionize more ionic species than NaCl, and hence has a higher osmotic pressure in view of the colligative property of osmotic pressure. Even though Li-Bet-Tf_2N and $MgCl_2$ ionize possess the same number of particle theoretically based on their formulas, Li-Bet-Tf_2N fails to produce a similar osmotic pressure to that of $MgCl_2$. This may be because Li-Bet-Tf_2N which has a large molecular structure easily forms ion pairs than small $MgCl_2$ molecule, resulting in a little lower osmotic pressure.

The relative viscosity of all draw solutes increases with their concentration with that of Li-Bet-Tf_2N having the largest increment (Fig. 2(b)). This is also related to the largest molecular structure of Li-Bet-Tf_2N. Nevertheless, Li-Bet-Tf_2N has relative viscosity lower than 1.9 at all studied concentrations, which is much lower than that of draw solutes reported recently, such as 2,3-expoxypropyl-trimethylammonium chloride (ETAC) [34], glycerol-oligo (ethyleneoxide)-block-oligo(butylene oxide) polymers (GE_7B_3) [35], poly(sodium styrene-4-sulfonate-*co*-n-*iso*-propyla crylamide) (PSSS-PNIPAM) [36], poly (aspartic acid sodium salt) (PAspNa) [37], gluconate salts [38] and other substances [39,40] yet along with a higher osmotic pressure (Table 1). Compared to those substances, Li-Bet-Tf_2N is more ionic with a smaller structure, which leads to a higher osmotic pressure and lower viscosity.

3.3 FO performance

The FO performance of Li-Bet-Tf_2N as a draw solute is comprehensively evaluated and compared with that of NaCl and $MgCl_2$ to identify the pros and cons of Li-Bet-Tf_2N in FO separation. The tests have been done in both pressure retarded osmosis (PRO, draw solution facing the membrane active layer) and FO (draw solution facing the porous substrate) modes. Figure 3 indicates that the water flux of Li-Bet-Tf_2N increases from 4.0 to 21.3 $L\cdot(m^2\cdot h)^{-1}$ in PRO mode and from 2.7 to 17.3 $L\cdot(m^2\cdot h)^{-1}$ in FO mode when the concentration is enhanced from 0.2 to 1.0 $mol\cdot L^{-1}$ (Figs. 3(a) and 3(b)). According to Fig. 2(a), the osmotic pressure of Li-Bet-Tf_2N is linearly increased with the concentration, thereby an increased net driving force across the membrane with Li-Bet-Tf_2N concentration and achieving a higher water flux. The water flux of the PRO mode is consistently higher than that with the FO mode. Li-Bet-Tf_2N may be entrapped in the membrane interior when facing the porous substrate side, that is, the FO mode, thus causing internal concentration polarization (ICP) which detrimentally impacts the FO process and leading to a lower water flux. This phenomenon is also widely observed elsewhere [41]. Nevertheless, Li-Bet-Tf_2N outperforms NaCl and is comparable to $MgCl_2$ in FO water permeation flux at the same experimental conditions (Figs. 3(a) and 3(b)). This may be because Li-Bet-Tf_2N has a large molecular structure which makes it less easily causing concentration polarization and diffusing to the feed side compared to NaCl and $MgCl_2$.

More remarkably, Li-Bet-Tf_2N has a smaller loss ($J_s\cdot J_w^{-1}$, $g\cdot L^{-1}$) than NaCl and $MgCl_2$ in the FO process (Figs. 3(a) and 3(b)). This is largely because the hydration ion radii of the solute particles in both NaCl and $MgCl_2$ fall in the size distribution of the PA FO membrane [42,43]. The severe salt fluxes of NaCl and $MgCl_2$ when used as draw solutes are also observed in other FO systems reported elsewhere [44,45]. The high salt flux of NaCl and $MgCl_2$ aggravates concentration polarization in the FO process and further reduce the water recovery efficiency [46,47]. In contrast, Li-Bet-Tf_2N shows a smaller loss. There are plenty of free oxygen atoms in both the cation and anion of Li-Bet-Tf_2N which allow the Li-Bet-Tf_2N aqueous system to form a large network with water molecules through hydrogen-bonding (Fig. 3(c)). As a result, the hydrated radius of Li-Bet-Tf_2N (20.1 nm) is much larger than the mean pore size of the membrane (0.3 nm) (Fig. 3(d)), achieving a smaller solute loss.

Compared with the aforementioned recently proposed draw solutes, ETAC [34], GE_7B_3 [35], PSSS-PNIPAM [36], PAspNa [37], gluconate salts [38] and other substances [39,40], Li-Bet-Tf_2N induces a significantly

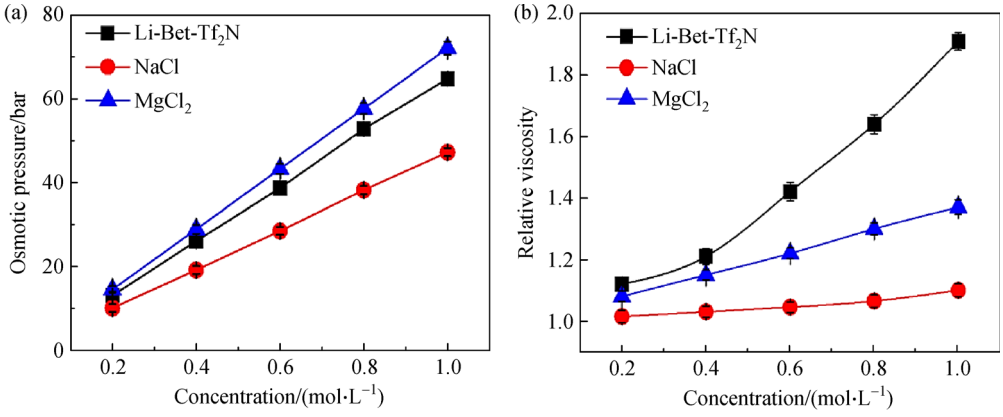

Fig. 2 (a) The osmotic pressure of Li-Bet-Tf_2N, NaCl and $MgCl_2$; (b) the relative viscosity of Li-Bet-Tf_2N, NaCl and $MgCl_2$ at 25 °C.

Table 1 A comparison in osmotic pressure and relative viscosity between Li-Bet-Tf_2N and other reported draw solutes at 25 °C

Compound	Concentration	Osmotic pressure/bar	Relative viscosity	Ref.
ETAC	20 wt-%	12.0	131.9	[34]
GE_3B_7	56 wt-%	15.0	62.7	[35]
PSSS-PNIPAM	33.3 wt-%	52.0	76.0	[36]
PAspNa	0.3 $g \cdot mL^{-1}$	51.5	4.4	[37]
Gluconate	0.4 $mol \cdot L^{-1}$	11.0	1.2	[38]
Li-Bet-Tf_2N	1.0 $mol \cdot L^{-1}$	64.5	1.9	This work

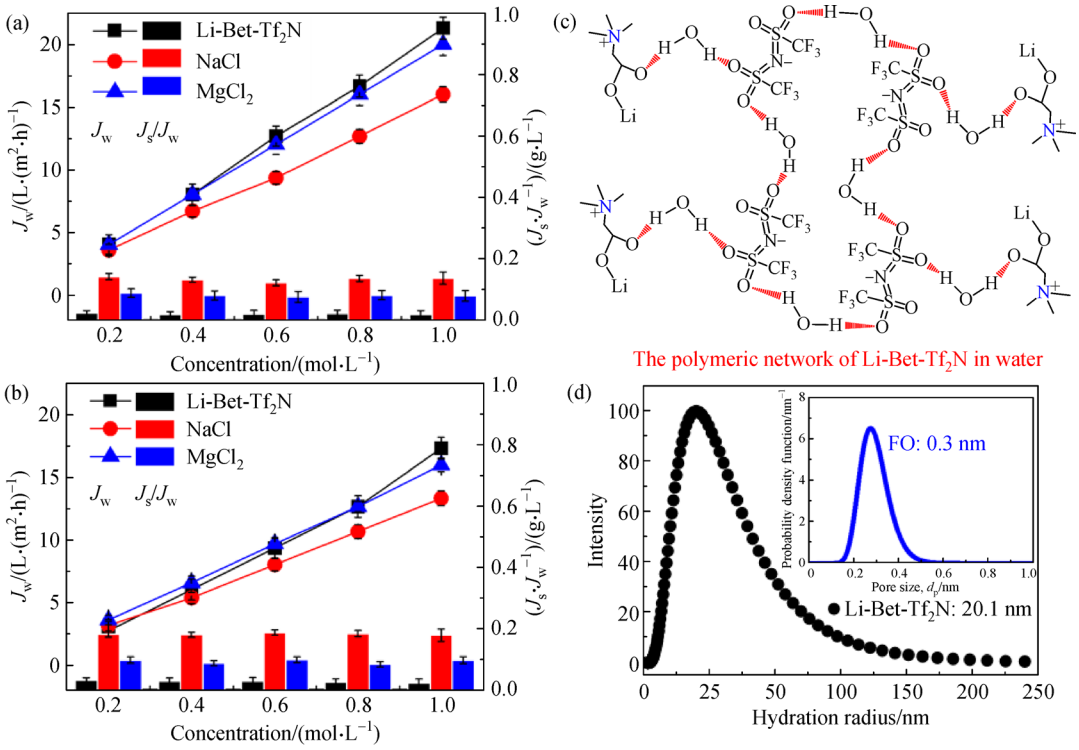

Fig. 3 FO performance comparison between Li-Bet-Tf_2N and the conventional draw solutes at room temperature: (a) under the PRO mode; (b) under the FO mode; (c) the polymeric network of Li-Bet-Tf_2N in water; (d) size distribution of the Li-Bet-Tf_2N polymeric network and FO membrane.

higher water flux with a comparable or lower solute loss during FO separation (Table 2). This is consistent with their osmotic pressure and inversely proportional to their viscosity (Table 1), and has a reasonable hydrated size to inhibit solute leakage (Fig. 3(c)). Thus Li-Bet-Tf_2N draw solute not only has a higher water recovery efficiency, but also avoids contamination to the feed solution and reduces the costs of draw solute replenishment as well. Therefore, Li-Bet-Tf_2N as a novel class of draw solute has great potentials in FO applications.

3.4 Li-Bet-Tf_2N draw solute in Li^+-containing wastewater purification

The application of Li-Bet-Tf_2N as a draw solute is evaluated in Li^+-containing wastewater purification through the FO process. Li_2SO_4 solution with the concentration of 0–2000 $mg \cdot L^{-1}$ is used as feed solution to simulate Li^+-containing wastewater. 1.0 $mol \cdot L^{-1}$ Li-Bet-Tf_2N serves as the draw solution, NaCl and $MgCl_2$ as conventional draw solutes have also been investigated for comparison (Fig. 4).

Regardless of the operation under the FO or PRO modes, a constant decline in water flux is observed when gradually elevating the feed concentration from 0 to 2000 $mg \cdot L^{-1}$ (Figs. 4(a) and 4(b)). A steady increase in osmotic pressure on the feed side is achieved with the feed concentration increase. That results in a reduced driving force of the FO separation process, leading to a reduced water flux. Consistent with the observations where deionized water as the feed, the water fluxes under the PRO mode surpass those with the FO mode for Li-Bet-

Table 2 FO performance comparison between Li-Bet-Tf_2N and other draw solutes at the best concentration

Compound	Concentration	Water flux/$(L\cdot(m^2\cdot h)^{-1})$	$(J_s\cdot J_w^{-1})/(g\cdot L^{-1})$	Ref.
ETAC	30 wt-%	2.9	0.39	[34]
GE_3B_7	56 wt-%	4.8	0.28	[35]
PSSS-PNIPAM	33.3 wt-%	4.0	0.5	[36]
PAspNa	0.3 $g\cdot mL^{-1}$	16.0	0.19	[37]
Gluconate	0.4 $mol\cdot L^{-1}$	6.0	0.17	[38]
Li-Bet-Tf_2N	1.0 $mol\cdot L^{-1}$	21.3	0.02	This work

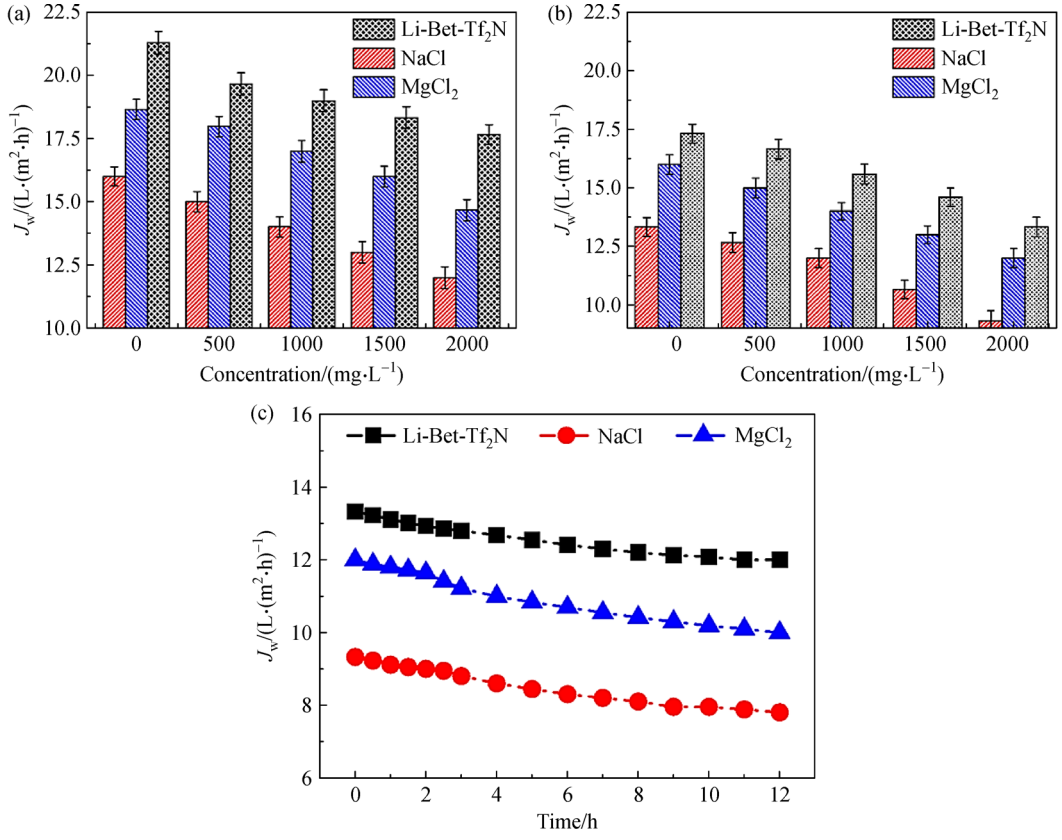

Fig. 4 FO short-term (30 min) performance at room temperature with 0–2000 $mg\cdot L^{-1}$ Li_2SO_4 as feed solutions and 1.0 $mol\cdot L^{-1}$ NaCl, $MgCl_2$ and Li-Bet-Tf_2N as draw solution, in Li^+ removal: (a) under the PRO mode; (b) under the FO mode; (c) the change of water flux in FO long-term (12 h) experiments under the FO mode at room temperature with 2000 $mg\cdot L^{-1}$ Li_2SO_4 as feed solutions and 1.0 $mol\cdot L^{-1}$ NaCl, $MgCl_2$ and Li-Bet-Tf_2N as draw solution.

Tf_2N due to the presence of ICP in the latter. Nevertheless, regardless of the feed concentration and membrane orientation, Li-Bet-Tf_2N outperforms both the NaCl and $MgCl_2$ draw solutes in extracting water from the Li^+-containing feed solution. These small inorganic salts have severe salt leakage (Figs. 3(a) and 3(b)). This not only causes a reduction in osmotic pressure on the draw solution side and an increase on the feed side, but also enhances the possibility of ICP occurrence, all leading to a decline in water flux. By contrast, Li-Bet-Tf_2N has negligible reverse diffusion in the course of FO separation, avoiding the above issues and hence producing a higher water permeation flux.

To evaluate the efficiency and stability of Li-Bet-Tf_2N in wastewater reclamation, we extend the experimental duration to 12 h in the FO purification of 2000 $mg\cdot L^{-1}$ Li_2SO_4 solution under the FO mode. The water fluxes of Li-Bet-Tf_2N, NaCl and $MgCl_2$ are reduced by 10.0%, 16.7% and 16.4%, respectively, compared to their initial values obtained in 30 min (Fig. 4(c)). As a result, Li-Bet-Tf_2N obtains an average water flux of 12.5 $L\cdot(m^2\cdot h)^{-1}$, 32.8% and 13.6% higher than those of NaCl and $MgCl_2$ respectively, suggesting higher water recovery efficiency and better sustainability of Li-Bet-Tf_2N than the conventional NaCl and $MgCl_2$ draw solutes in FO water treatment.

One more advantage of using Li-Bet-Tf_2N over NaCl or $MgCl_2$ to purify the Li^+-containing wastewater is that Li-Bet-Tf_2N solves the issue of Li^+ reverse diffusion from the feed to the draw solution side. The Li^+ ion in the feed solution has a hydrated radius of 0.38 nm which is comparable to that of the pore size of the PA membrane used here [42,43]. Consequently, the Li_2SO_4 feed solute diffuses to the draw solution during the FO process which is experimentally confirmed. When using 2000 $mg \cdot L^{-1}$ Li_2SO_4 as the feed solution and 1.0 $mol \cdot L^{-1}$ $MgCl_2$ as the draw solution which produces a water flux comparable to that of 1.0 $mol \cdot L^{-1}$ Li-Bet-Tf_2N, 22.1 mg of Li^+ is detected on the draw solution side after 12 h FO tests based on the ICP-OES analysis. The observation shows that the draw solution will be polluted in the FO process when treating Li^+-containing wastewater. Nevertheless, this problem can be tackled effectively with Li-Bet-Tf_2N as the draw solute. According to Fig. 1(a), Li^+ ions readily react with [Hbet][Tf_2N] ionic liquid to give Li-Bet-Tf_2N. As such, the Li^+ diffusing from the feed side is conveniently converted to Li-Bet-Tf_2N by reacting with a stoichiometric amount of [Hbet][Tf_2N] which is added to the Li-Bet-Tf_2N solution after FO tests. This not only avoids contamination of draw solution, but also partly replenishes the loss of draw solute which is inevitable in FO operation, suggesting Li-Bet-Tf_2N an ideal draw solute for FO Li^+-containing wastewater purification.

3.5 Recovery and reuse of Li-Bet-Tf_2N

Li-Bet-Tf_2N is easily recycled through [Hbet][Tf_2N] solvent extraction after FO experiments (Fig. 5). As Li-Bet-Tf_2N is much more soluble in [Hbet][Tf_2N] than in water, adding [Hbet][Tf_2N] to the dilute Li-Bet-Tf_2N solution (Fig. 5(a)) extracts the solute to the [Hbet][Tf_2N] organic phase from its aqueous solution which stays under the water phase (Fig. 5(b)). Thus the water in the upper layer is separated easily. Diluted HCl is then added to the [Hbet][Tf_2N] phase to decompose Li-Bet-Tf_2N into [Hbet][Tf_2N] and LiCl which dissolves in the upper aqueous phase (Fig. 5(c)). After that, [Hbet][Tf_2N] is separated for reuse. Na_2CO_3 is added to convert LiCl to Li_2CO_3 precipitate. Li-Bet-Tf_2N is finally obtained (Fig. 5 (a)) through the reaction illustrated in Fig. 1(a). Compared to the recycling of other synthetic draw solutes which have been achieved via either thermal process [48,49], pressure-driven separation [37], environmental stimuli [50] or other energy intensive approaches [20,51], the recovery of Li-Bet-Tf_2N is more facile and efficient without energy input, organic solvent involved and by-products produced. The recycled Li-Bet-Tf_2N is re-characterized by ^1H NMR, FTIR diffraction and re-evaluated through FO separation. Reproducible results have been obtained, demonstrating the good stability and reusability of Li-Bet-Tf_2N as an FO draw solute.

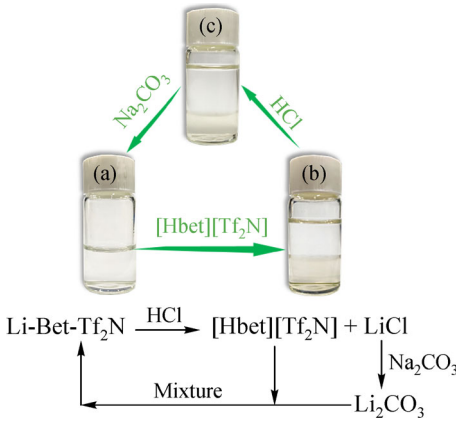

Fig. 5 Recycling of Li-Bet-Tf_2N via solvent extraction: (a) the aqueous solution of Li-Bet-Tf_2N; (b) Li-Bet-Tf_2N in the mixed solvents (water in the upper layer while Li-Bet-Tf_2N and [Hbet][Tf_2N] in the lower layer); (c) LiCl in the upper aqueous layer, while [Hbet][Tf_2N] in the lower layer is easily recycled.

4 Conclusions

A novel Li-Bet-Tf_2N draw solute is synthesized via a simple one-pot reaction from Li_2CO_3 recovered from LIB waste and a plant-derived compound, betaine. Li-Bet-Tf_2N outperforms the conventional NaCl and $MgCl_2$ draw solutes with a higher water flux and smaller solute losses. Li-Bet-Tf_2N is more suitable to purify Li^+-containing wastewater by tackling the Li^+ reverse diffusion issue and is easily recovered after FO via solvent extraction. The recycled Li-Bet-Tf_2N can be repeatedly used for FO separation, showing great potentials in FO application.

Acknowledgements We thank the financial supports from the National Natural Science Foundation of China (Grant No. 21677035) and the Natural Science Foundation of Fujian Province (Grant No. 2021J01629).

References

1. Mu T, Zuo P, Lou S, Pan Q, Li Q, Du C, Gao Y, Cheng X, Ma Y, Yin G. A two dimensional nitrogen-rich carbon/silicon composite as high performance anode material for lithium ion batteries. Chemical Engineering Journal, 2018, 341: 37–46
2. Chen H, Wang S, Liu X, Hou X, Chen F, Pan H, Qin H, Lam K H, Xia Y, Zhou G. Double-coated Si-based composite composed with carbon layer and graphene sheets with void spaces for lithium-ion batteries. Electrochimica Acta, 2018, 288: 134–143
3. Wu J, Liu J, Wang Z, Gong X, Wang Y. A new design for Si wears double jackets used as a high-performance lithium-ion battery anode. Chemical Engineering Journal, 2019, 370: 565–572
4. Chen H, He S, Hou X, Wang S, Chen F, Qin H, Xia Y, Zhou G. Nano-Si/C microsphere with hollow double spherical interlayer and submicron porous structure to enhance performance for lithium-ion battery anode. Electrochimica Acta, 2019, 312: 242–250
5. Zhou Y, Hou X, Shen K, Wang S, Chen F, Li Y, Chen H, Wang B.

$Li_{1.1}Na_{0.1}Mn_{0.53}4Ni_{0.133}Co_{0.133}O_2$ as cathode with ameliorated electrochemical performance based on dual Li^+/Na^+ electrolyte. Ionics, 2018, 25(1): 51–59
6. Miser H D, Stevens R E, Ogunseitan O A. Potential environmental and human health impacts of rechargeable lithium batteries in electronic waste. Environmental Science & Technology, 2013, 47(10): 5495–5503
7. Mao X, Wong A A, Crawford R W. Cobalt toxicity—an emerging clinical problem in patients with metal-on-metal hip prostheses. Medical Journal of Australia, 2011, 194(12): 649–651
8. Zhang Y, Cheng X, Jiang X, Urban J J, Lau C H, Liu S, Shao L. Robust natural nanocomposites realizing unprecedented ultrafast precise molecular separations. Materials Today, 2020, 36: 40–47
9. Tang M J, Liu M L, Wang D A, Shao D D, Wang H J, Cui Z L, Cao X L, Sun S P. Precisely patterned nanostrand surface of cucurbituril [n]Based nanofiltration membranes for effective alcohol-water condensation. Nano Letters, 2020, 20(4): 2717–2723
10. Song J, Nghiem L, Li X M, He T. Lithium extraction from Chinese salt-lake brines: opportunities, challenges, and future outlooks. Environmental Science. Water Research & Technology, 2017, 3(4): 593–597
11. Luo X, Zhang K, Luo J, Luo S, Crittenden J. Capturing lithium from wastewater using a fixed bed packed with 3-D MnO_2 ion cages. Environmental Science & Technology, 2016, 50(23): 13002–13012
12. Ge Q, Chung T S. Oxalic acid complexes: promising draw solutes for forward osmosis (FO) in protein enrichment. Chemical Communications, 2015, 51(23): 4854–4857
13. Han G, Liang C Z, Chung T S, Weber M, Staudt C, Maletzko C. Combination of forward osmosis (FO) process with coagulation/flocculation (CF) for potential treatment of textile wastewater. Water Research, 2016, 91: 361–370
14. Dong X, Ge Q. Metal ion-bridged forward osmosis membranes for efficient pharmaceutical wastewater reclamation. ACS Applied Materials & Interfaces, 2019, 11(40): 37163–37171
15. Liu M L, Li L, Sun Y X, Fu Z J, Cao X L, Sun S P. Scalable conductive polymer membranes for ultrafast organic pollutants removal. Journal of Membrane Science, 2021, 617: 118644
16. Zhang Y, Guo J, Han G, Bai Y, Ge Q, Ma J, Lau C H, Shao L. Molecularly soldered covalent organic frameworks for ultrafast precision sieving. Science Advances, 2021, 7(13): eabe8706
17. Wang Z Y, Fu Z J, Shao D D, Lu M J, Xia Q C, Xiao H F, Su B W, Sun S P. Bridging the miscibility gap to fabricate delamination-free dual-layer nanofiltration membranes via incorporating fluoro substituted aromatic amine. Journal of Membrane Science, 2020, 610: 118270
18. Han G, de Wit J S, Chung T S. Water reclamation from emulsified oily wastewater via effective forward osmosis hollow fiber membranes under the PRO mode. Water Research, 2015, 81: 54–63
19. Mondal P, Tran A T K, der Bruggen B V. Removal of As(V) from simulated groundwater using forward osmosis: effect of competing and coexisting solutes. Desalination, 2014, 348: 33–38
20. Ge Q, Su J, Amy G L, Chung T S. Exploration of polyelectrolytes as draw solutes in forward osmosis processes. Water Research, 2012, 46(4): 1318–1326
21. Zhao Q, Chen N, Zhao D, Lu X. Thermoresponsive magnetic nanoparticles for seawater desalination. ACS Applied Materials & Interfaces, 2013, 5(21): 11453–11461
22. Fan X, Liu H, Gao Y, Zou Z, Craig V S J, Zhang G, Liu G. Forward-osmosis desalination with poly(ionic liquid) hydrogels as smart draw agents. Advanced Materials, 2016, 28(21): 4156–4161
23. Zhong Y, Wang X, Feng X, Telalovic S, Gnanou Y, Huang K W, Hu X, Lai Z. Osmotic heat engine using thermally responsive ionic liquids. Environmental Science & Technology, 2017, 51(16): 9403–9409
24. Dutta D, Kumari A, Panda R, Jha S, Gupta D, Goel S, Jha M K. Close loop separation process for the recovery of Co, Cu, Mn, Fe and Li from spent lithium-ion batteries. Separation and Purification Technology, 2018, 200: 327–334
25. Chen X, Ma H, Luo C, Zhou T. Recovery of valuable metals from waste cathode materials of spent lithium-ion batteries using mild phosphoric acid. Journal of Hazardous Materials, 2017, 326: 77–86
26. Nockemann P, Thijs B, Hecke K V, Meervelt L V, Binnemans K. Polynuclear metal complexes obtained from the task-specifific ionic liquid betainium bistriflimide. Crystal Growth & Design, 2008, 8(4): 1353–1363
27. Wu Y, Zhang W, Ge Q. Piperazine-based functional materials as draw solutes for desalination via forward osmosis. ACS Sustainable Chemistry & Engineering, 2018, 6(11): 14170–14177
28. Liao X, Zhang W, Ge Q. A cage-like supramolecular draw solute that promotes forward osmosis for wastewater remediation and source recovery. Journal of Membrane Science, 2020, 600: 117862
29. Meng J, Lau C H, Xue Y, Zhang R, Cao B, Li P. Compatibilizing hydrophilic and hydrophobic polymers via spray coating for desalination. Journal of Materials Chemistry. A, Materials for Energy and Sustainability, 2020, 8(17): 8462–8468
30. Stone M L, Wilson A D, Harrup M K, Stewart F F. An initial study of hexavalent phosphazene salts as draw solutes in forward osmosis. Desalination, 2013, 312: 130–136
31. Razmjou A, Simon G P, Wang H. Effect of particle size on the performance of forward osmosis desalination by stimuli-responsive polymer hydrogels as a draw agent. Chemical Engineering Journal, 2013, 215: 913–920
32. Zhang Y, Yang L, Pramoda K P, Gai W, Zhang S. Highly permeable and fouling resistant hollow fiber membranes for reverse osmosis. Chemical Engineering Science, 2019, 207: 903–910
33. Brzezinski B, Olejnik J, Zundel G, Kramer R. Intramolecular $O^-Li^+\ldots ON \rightleftharpoons O^-\ldots Li^+ON$ bonds with large Li^+ polarizability. Chemical Physics Letters, 1989, 156(2-3): 213–217
34. Laohaprapanona S, Fub Y J, Hua C C, Youc S J, Tsaia H A, Hunga W S, Leea K R, Lai J Y. Evaluation of a natural polymer-based cationic polyelectrolyte as a draw solute in forward osmosis. Desalination, 2017, 421: 72–78
35. Inada A, Yumiya K, Takahashi T, Kumagai K, Hashizume Y, Matsuyam H. Development of thermoresponsive star oligomers with a glycerol backbone as the draw solute in forward osmosis process. Journal of Membrane Science, 2019, 574: 147–153
36. Zhao D, Wang P, Zhao Q, Chen N, Lu X. Thermoresponsive copolymer-based draw solution for seawater desalination in a combined process of forward osmosis and membrane distillation. Desalination, 2014, 348: 26–32
37. Gwak G, Jung B, Han S, Hong S. Evaluation of poly (aspartic acid sodium salt) as a draw solute for forward osmosis. Water Research,

2015, 80: 294–305
38. Long Q, Qi G, Wang Y. Evaluation of renewable gluconate salts as draw solutes in forward osmosis process. ACS Sustainable Chemistry & Engineering, 2016, 4(1): 85–93
39. Wang Z, Wu S, He Z. Production of electricity and water in an osmotic microbial fuel cell by using EDTA-2Na as a recoverable draw solute. Science of the Total Environment, 2019, 677: 382–389
40. Hsu C H, Ma C, Bui N, Song Z, Wilson A D, Kostecki R, Urban J J. Enhanced forward osmosis desalination with a hybrid ionic liquid/hydrogel thermoresponsive draw agent system. ACS Omega, 2019, 4(2): 4296–4303
41. Heikkinen J, Kyllönen H, Järvelä E, Grönroos A, Tang C Y. Ultrasound-assisted forward osmosis for mitigating internal concentration polarization. Journal of Membrane Science, 2017, 528: 147–154
42. Xu W, Ge Q. Synthetic polymer materials for forward osmosis (FO) membranes and FO applications: a review. Reviews in Chemical Engineering, 2019, 35(2): 191–209
43. Volkov A G, Paula S, Deamer D W. Two mechanisms of permeation of small neutral molecules and hydrated ions across phospholipid bilayers. Bioelectrochemistry and Bioenergetics, 1997, 42(2): 153–160
44. Behboudia A, Ghiasia S, Mohammadia T, Ulbricht M. Preparation and characterization of asymmetric hollow fiber polyvinyl chloride (PVC) membrane for forward osmosis application. Separation and Purification Technology, 2021, 270(1): 118801
45. Sun P, Jang Y, Ham S, Ryoo H S, Park H D. Effects of reverse solute diffusion on membrane biofouling in pressure-retarded osmosis processes. Desalination, 2021, 512(15): 115145
46. She Q, Hou D, Liu J, Tan K H, Tang C Y. Effect of feed spacer induced membrane deformation on the performance of pressure retarded osmosis (PRO): implications for PRO process operation. Journal of Membrane Science, 2013, 445: 170–182
47. She Q, Wang R, Fane A G, Tang C Y. Membrane fouling in osmotically driven membrane processes: a review. Journal of Membrane Science, 2016, 499: 201–233
48. Xu W, Ge Q. Novel functionalized forward osmosis (FO) membranes for FO desalination: improved process performance and fouling resistance. Journal of Membrane Science, 2018, 555: 507–516
49. Ge Q, Lau C H, Liu M. A novel multi-charged draw solute that removes organic arsenicals from water in a hybrid membrane process. Environmental Science & Technology, 2018, 52(6): 3812–3819
50. Wu Y, Liu Y, Chen R, Zhang W, Ge Q. A pH-responsive supramolecular draw solute that achieves high-performance in arsenic removal via forward osmosis. Water Research, 2019, 165: 114993
51. Ding C, Zhang X, Xiong S, Shen L, Yi M, Liu B, Wang Y. Organophosphonate draw solution for produced water treatment with effectively mitigated membrane fouling via forward osmosis. Journal of Membrane Science, 2020, 593: 117429